SPATIALLY-VARYING OUT-OF-FOCUS IMAGE DEBLURRING WITH L1-2 OPTIMIZATION AND A GUIDED BLUR MAP

Chih-Tsung Shen [1,2], *Wen-Liang Hwang* [2], *and Soo-Chang Pei* [1,3]

[1] Graduate Institute of Networking and Multimedia, National Taiwan University, Taipei, 106 Taiwan
[2] Institute of Information Science, Academia Sinica, Taipei, 115 Taiwan, R.O.C.
[3] Department of Electrical Engineering, National Taiwan University Taipei, 106 Taiwan, R.O.C.
E-mail: shenchihtsung@gmail.com, whwang@iis.sinica.edu.tw, pei@cc.ee.ntu.edu.tw

ABSTRACT

In this paper, we propose a spatially-varying deblurring method to remove the out-of-focus blur. Our proposed method mainly contains three parts: blur map generation, image deblurring, and scale selection. First, we derive a blur map using local contrast prior and the guided filter. Second, we propose our image deblurring method with L1-2 optimization to obtain a better image quality. Finally, we adopt the scale selection to ensure our output free from ringing artifacts. The experimental results demonstrate our proposed method is promising.

Index Terms— out-of-focus blur, spatially-varying deblurring, L1-2 optimization, guided blur map.

1. INTRODUCTION

In the past decade, digital photographs become necessities in our daily life, especially as digital cameras and camera phones are widely used. Due to the physical requirement, photographs have some trade-offs between exposure-time, aperture-size, and depth-of-field during image acquisition. Although a longer exposure-time can guarantee the image sensors to capture enough light, the photograph taken by a longer exposure-time may lead to a motion-blurred image and hard to be reconstructed[1]. On the other hand, although using a bigger aperture can prevent the motion-blur and capture enough light, the out-of-focus blur and the limited depth-of-field become the main drawbacks. In this paper, we propose a software-based method to remove the spatially-varying out-of-focus blur while extend the depth-of-field.

In 2007, Bae et al. calculated the second derivatives of input image to extract the blur scale on edge. They also borrowed the colorization method to propagate the blur scale and obtain a 2-D blur map (defocus map). However, the colorization method cannot grantee a correct blur map, Bae et al.'s method is not sufficient for image reconstruction[2]. In 2009, Tai et al. obtained their blur map by using their local contrast prior. They did not estimate the in-focus parameter so as to require an interactive input for their blur map[3].

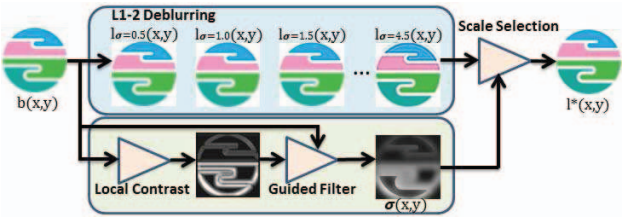

Fig. 1. Flowchart of our proposed method. We reconstruct $l^*(x, y)$ from a spatially-varying blurry input $b(x, y)$ by using blur map generation, L1-2 Deblurring, and scale selection.

In 2011, Trentacoste et al. estimated their blur map by comparing the edges inside the scale-space of the input image. They proposed their idea for blur-aware down-sampling, not for image reconstruction. Kee et al. proposed their spatially-varying deblurring for optical blur, but they did not deal with the problems caused by the out-of-focus blur[4]. Besides, Zhuo et al. re-blurred the image to extract the blur scale on edges. They presented their blur map and the results for defocus magnification, but they did not show the all-in-focus results[5].

Our proposed method can be viewed as three parts. First, we estimate our blur map by combining the modified local contrast prior and the guided filter. Second, we deblur the whole out-of-focus blurry input with L1-2 optimization scale by scale, and obtain a set of deblurred images as the candidates of our output. In the last step, according to our blur map, we select the deblurred pixels to reconstruct our all-in-focus output image. The experimental results show that our proposed method outperforms than the existing space-invariant deblurring methods proposed by Shan et al.[6] and Xu et al.[7], respectively. Besides, our proposed method still outperforms than the spatially-varying method using the cascaded combination of Bae et al.'s blur map and Chan et al.'s image deblurring method[8].

2. OUR PROPOSED METHOD

We first estimate our blur map by using the modified local contrast prior and the guided filter. Second, we propose an image deblurring method optimized with both discrete total variation (TV) and Tikhonov-like regularizer. With this L1-2 optimization, we deblur the input image to obtain a set of deblurred images. In the final step, we adopt the scale selection to select the deblurred pixels to fill in the final all-in-focus output. The flowchart is show in Fig. 1 while the details are introduced as below:

2.1. Blur map generation

For the latent edge signal $l(x)$, we can model it as

$$l(x) = A \cdot u(x) + B \tag{1}$$

where $u(x)$ is the step function, A is the amplitude, B is the offset, and the edge is located at $x = 0$.

Suppose the edge signal $l(x)$ suffers the out-of-focus blur, we can approximate the blurry signal $b(x)$ as the convolution:

$$b(x) = l(x) \otimes g(x, \sigma) \tag{2}$$

where $g(x, \sigma)$ is the Gaussian function with its standard deviation σ:

$$g(x, \sigma) = \frac{1}{\sqrt{2\pi}\sigma} exp(-\frac{x^2}{2\sigma}) \tag{3}$$

In order to extract the blur scale σ, we reference the local contrast prior $LC(x)$ proposed in [3] and then modify it using the edge properties derived from [5]. Following the previous equations, we can obtain the gradient of the blurry edge and then substitute it into $LC(x)$. We have

$$\nabla b(x) = \nabla(l(x) \otimes g(x, \sigma)) = A \cdot g(x, \sigma) \tag{4}$$

and

$$LC(x) = \frac{\max|\nabla b(x')|}{\max b(x') - \min b(x')} \tag{5}$$

$$\approx \frac{1}{\sqrt{2\pi}\sigma} \max|\exp(-\frac{x^2}{2\sigma^2})| \tag{6}$$

where x' is the neighborhood of x.

Since $\max|\exp(0)| = 1$ at the edge location ($x = 0$), we can easily adopt $|\nabla b(x, y)| = \sqrt{\nabla b_x^2 + \nabla b_y^2}$ from x- and y-directions to obtain our 2-D blur map as follows:

$$\sigma(x, y) = \frac{1}{\sqrt{2\pi} LC(x, y)} = \frac{0.3989}{LC(x, y)} \tag{7}$$

where $LC(x, y) = \frac{\max|\nabla b(x', y')|}{\max b(x', y') - \min b(x', y')}$ and (x', y') is the neighborhood of (x, y) within a local window.

Moreover, in order to remove the ambiguity around edges and the noise of our blur map, we adopt the original blur image as the guided image to lead us to a better blur map after guided filtering [9].

$$\sigma(x, y) \leftarrow GF\{b(x, y), \sigma(x, y), r, \epsilon\} \tag{8}$$

2.2. Image deblurring with L1-2 optimization

After generating the blur map, we propose our image deblurring method with L1-2 optimization to obtain the deblurred images for all-in-focus image reconstruction.

Our image deblurring with L1-2 optimization adopts both Tikhonov-like regularizer and TV regularizer. Consider b be the blurry image, G_σ represent a Gaussian blurring operator with blur scale σ, l_σ be the corresponding deblurred $n \times n$ gray-scale image, and r be additive noise.

$$b = G_\sigma l_\sigma + r \tag{9}$$

Since b is the input blurry image, b is given. Suppose G_σ is determined, we can recover l_σ using our proposed model:

$$\min_{l_\sigma} \frac{\mu}{2}\|G_\sigma l_\sigma - b\|_2^2 + \alpha \cdot \sum_{i=1}^{n^2} \|D_i l_\sigma\| + (1-\alpha) \cdot \sum_{i=1}^{n^2} \|D_i l_\sigma\|_2^2 \tag{10}$$

where $D_i l_\sigma$ denotes the discrete gradient of l_σ at pixel i, $\sum \|D_i l_\sigma\|$ is the TV regularizer of l_σ, and $\sum \|D_i l_\sigma\|_2^2$ is the Tikhonov-like regularizer. Besides, μ is a parameter, and $0 \le \alpha \le 1$.

Similar to Wang et al's [10], we adopt variable-splitting and penalty techniques for our L1-2 optimization. At each pixel, we introduce an auxiliary variable w_i to transfer $D_i l_\sigma$ outside the non-differentiable term $\|\cdot\|$ and penalize the difference between w_i and $D_i l_\sigma$. We can yield the approximation model as follows:

$$\min_{w, l_\sigma} \frac{\mu}{2}\|G_\sigma l_\sigma - b\|_2^2 \tag{11}$$
$$+ \alpha \cdot (\sum_{i=1}^{n^2} \|w_i\| + \frac{\beta}{2} \sum_{i=1}^{n^2} \|w_i - D_i l_\sigma\|_2^2) + (1-\alpha) \cdot \sum_{i=1}^{n^2} \|D_i l_\sigma\|_2^2$$

with a large enough penalty parameter β such that $w_i \to D_i l_\sigma$ and the minimization question described in equation (11) is modified into a penalty function in degree (w, l_σ).

We adopt an alternating minimization algorithm to minimize the penalty function with respect to either w_i and l_σ. For a fixed l_σ, only the middle two term related to w_i are separable with respect to w_i, so minimizing equation (11) is equivalent to solving the following equation:

$$\min_{w_i} \|w_i\| + \frac{\beta}{2} \sum_{i=1}^{n^2} \|w_i - D_i l_\sigma\|_2^2 \tag{12}$$

for which the unique solver is given using matrix calculus by the following formula:

$$w_i = \max\{\|D_i l_\sigma\| - \frac{1}{\beta}, 0\} \frac{D_i l_\sigma}{\|D_i l_\sigma\|} \tag{13}$$

where $i = 1, 2, \cdots, n^2$ and the convention $(0/0) = 0$. In the other hand, for a fixed w_i, we can easily minimize l_σ by solving the quadratic equation described in equation (14).

$$\min_{l_\sigma} \frac{\mu}{2}\|G_\sigma l_\sigma - b\|_2^2 + \frac{\alpha\beta}{2} \sum_{i=1}^{n^2} \|w_i - D_i l_\sigma\|_2^2 + (1-\alpha) \cdot \sum_{i=1}^{n^2} \|D_i l_\sigma\|_2^2 \tag{14}$$

To solve equation (14), we can obtain a closed-form solution:

$$(\frac{\mu}{2}G_\sigma^T G_\sigma + (\frac{\alpha\beta}{2} + 1 - \alpha)D_i^T D_i)l_\sigma = \frac{\alpha\beta}{2}D_i^T w_i + \frac{\mu}{2}G_\sigma^T b \tag{15}$$

Assume l_σ is under the periodic boundary condition, we have D_i and $G_\sigma^T G_\sigma$ are all block circulant. Therefore, we can utilize 2D discrete fourier transform F to replace the huge matrix calculation. Using the convolution theorem of Fourier transforms, we can obtain l_σ from the digital filter:

$$l_\sigma = \tag{16}$$
$$F^{-1}\{\frac{(\frac{\alpha\beta}{2})F(D_i)^* \circ F(w_i) + (\frac{\mu}{2})F(G_\sigma)^* \circ F(b)}{((\frac{\alpha\beta}{2}) + (1-\alpha))F(D_i)^* \circ F(D_i) + (\frac{\mu}{2})F(G_\sigma)^* \circ F(G_\sigma)}\}$$

where "$*$" denotes complex conjugacy, "$\circ$" denotes componentwise multiplication, and the division is also componentwise. In our alternating minimization algorithm, for given b, G_σ, α, β, and μ, we can
(i) initialize $b = l_\sigma$,
(ii) iteratively compute w according to equation (13) for fixed l_σ, and compute l_σ according to equation (16) for fixed w.
Until the minimizing penalty function reaches its convergence, we can obtain the final deblurred image l_σ. Using different blur scales, we can obtain N deblurred image candidates $\{l_{\sigma_1}, l_{\sigma_2}, \cdots, l_{\sigma_N}\}$for image reconstruction.

2.3. Scale Selection for image reconstruction

In previous subsection, we generate our blur map and obtain our deblurred images with L1-2 optimization. We quantize the continuous blur map to discrete blur scales from σ_1, σ_2, to σ_N with the step size q. Afterwards, we reconstruct our all-in-focus image as follows:

$$l^*(x,y) = \sum_{(x,y)} l_{\sigma^*(x,y)}(x,y) \tag{17}$$

where $\sigma^*(x,y)$ is the biggest quantized blur scale close to $\sigma(x,y)$. Since $\sigma^*(x,y) \leq \sigma(x,y)$, we can suppress the ringing artifacts which are caused by non-regularity [11].

3. EXPERIMENTAL RESULTS

First, we examine the performance of our image deblurring with L1-2 optimization. We use the following six images from USC SIPI database as reference images: Girl (Lena), Stream and bridge, Baboon, Man, Peppers, and f16. 2D Gaussian blur with standard variation (blur scale) set at 4 pixels is applied to the reference images. Then, we adopt TwIST [12], FTVd [10], deconvtv [8], and our L1-2 model to delur the blurred images with deblurring scales at 2, 4, 6, and 8 pixels. The parameters of our L1-2 method are set as follows: $\mu = 18$, $\alpha = 0.8$, and β is a updating parameter which its initial value equals 1. The performance is measured by SSIM and PSNR. From Figure 3, we can see that our L1-2 method has the same performance when the images are deblurred at

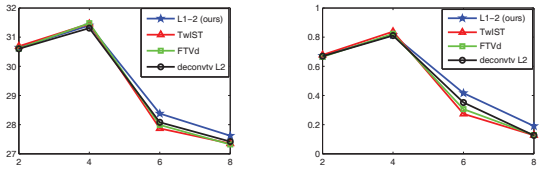

(a) PSNR (b) SSIM

Fig. 2. Comparison of the average performance of the four deblurring algorithms with different blurring scale estimation. The blue, green, red, and black curves correspond to our L1-2, FTVd [10], TwIST [12], and deconvtv [8], respectively.

the true blurring scale. We can also obverse that our L1-2 method outperforms than the compared methods when the blurring scale is incorrect (over-estimated).

Second, we adopt equation (7) to obtain the continuous blur map $\sigma(x,y)$ with a local window of size 11×11 and set $\gamma = 10$,$\epsilon = 0.01$ for guided image filtering. Afterwards, we quantize $\sigma(x,y)$ with the step size $q = 0.5$ pixels. Since our blur scales increase linearly from 0.5 pixels to 4.5 pixels, we have 9 different blurring scales within our quantized blur map $\sigma^*(x,y)$. Figure 3(a) shows the 'face' image captured using Nikon Camera Control Pro 2 to focus on the ball. The ball and two men range at different depth so as to suffer spatially-varying out-of-focus blur. Figure 3(b) is our guided blur map before quantization (dark pixel suffers small blurring scale, and vice versa). Figure 3(c) shows the all-in-focus result obtained by our method. Figure 3(d) is the result obtained using Bae et al.'s blur map and Chan et al.'s deconvtv model. Our method obtains sharper image without the ringing artifacts evident in Figure 3(c). Figure 4(a) shows the 'stone' image, which suffers spatially-varying blur. Figure 4(b) and 4(c) show our blur map and our all-in-focus result, respectively. Figure 4(d) is the result obtained by Xu et al.'s space-invariant image deblurring [7]. Our result extends the depth-of-field while outperforms Xu et al.'s result. Figure 5(a) shows the 'building' image, which suffers spatially-varying out-of-focus blur. The magnified regions shows that our result (Figure 5(h)) reconstruct both foreground and background while the other methods (Figure 5(i-k)) fail to reconstruct both foreground and background. Please visit: www.iis.sinica.edu.tw/ ∼ctshen/svDeblur/svDeblur.html

4. CONCLUSIONS

First, we estimate the blur map using the modified local contrast prior with the guided image filtering. Second, we propose an L1-2 deblurring model that is more robust than the TV model when the blurring kernel estimation is subject to errors. Finally, our all-in-focus results demonstrate that our spatially-varying deblurring method is promising as compared to the existing delurring methods.

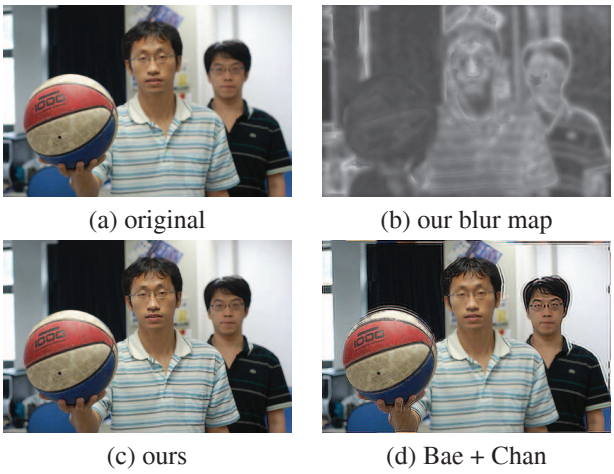

(a) original (b) our blur map

(c) ours (d) Bae + Chan

Fig. 3. (a) The original 'face' image, (b) our blur map (dark pixel suffers small blurring scale, and vice versa), (c) our all-in-focus result, and (d) the result using Bae et al.'s blur map and Chan et al.'s deconvtv.

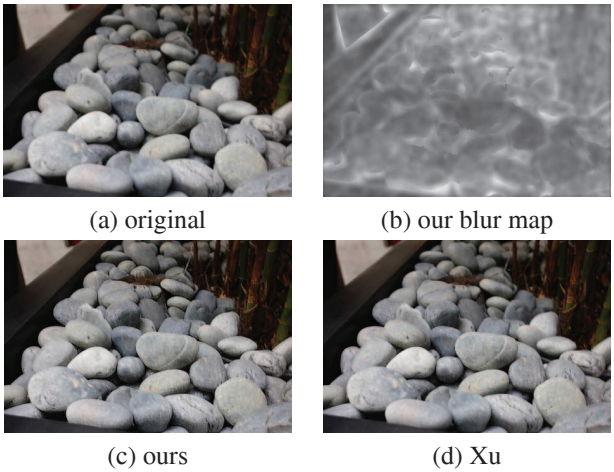

(a) original (b) our blur map

(c) ours (d) Xu

Fig. 4. (a) The original 'stone' image, (b) our blur map, (b) our all-in-focus result, and (d) Xu et al.'s result.

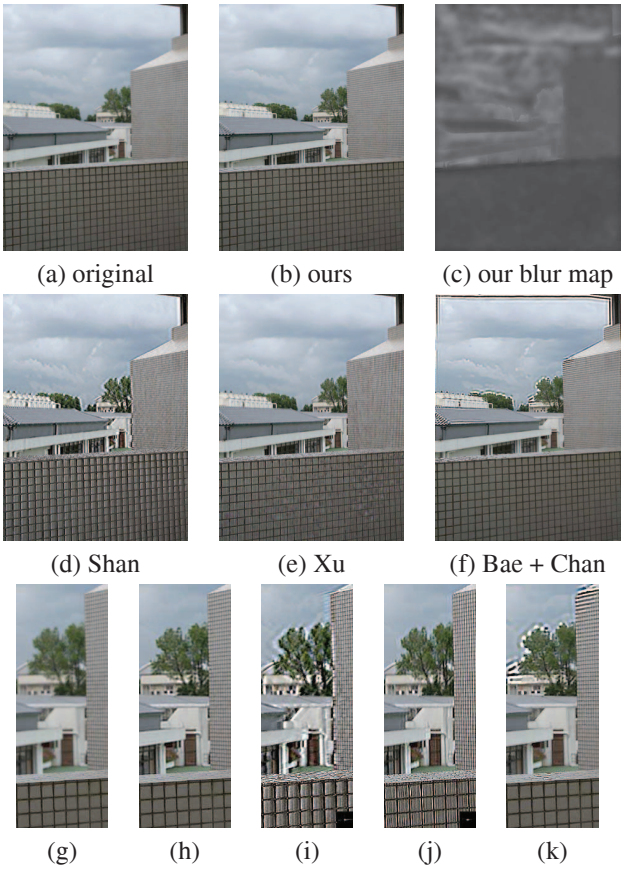

(a) original (b) ours (c) our blur map

(d) Shan (e) Xu (f) Bae + Chan

(g) (h) (i) (j) (k)

Fig. 5. (a) The original 'building' image, (b) our all-in-focus result, (c) our blur map,(d) Shan et al.'s result [6], (e) Xu et al.'s result, (f) the result using Bae et al.'s blur map and Chan et al.'s deconvtv, and (g-h) are the magnified regions of (a,b,d,e,f), respectively.

5. REFERENCES

[1] O. Whyte, J. Sivic, A. Zisserman, and J. Ponce, "Non-uniform deblurring for shaken images," in *CVPR*, 2010, pp. 491–498.

[2] S. Bae and F. Durand, "Defocus magnification," *Comput. Graph. Forum*, vol. 26(3), pp. 571–579, 2007.

[3] Y.-W. Tai and M. Brown, "Single image defocus map estimation using local contrast prior," in *ICIP*, 2009, pp. 1797–1800.

[4] E. Kee, S. Paris, S. Chen, and J. Wang, "Modeling and removing spatially-varying optical blur," in *ICCP*, 2011.

[5] S. Zhuo and T. Sim, "Defocus map estimation from a single image," *Pattern Recognition*, vol. 44(9), pp. 1852–1858, 2011.

[6] Q. Shan, J. Jia, and A. Agarwala, "High-quality motion deblurring from a single image," *ACM Trans. on Graphics*, vol. 27(3), 2008.

[7] L. Xu and J. Jia, "Two-phase kernel estimation for robust motion deblurring," in *ECCV*, 2010, pp. 157–170.

[8] S. Chan, R. Khoshabeh, K. Gibson, P. Gill, and T. Nguyen, "An augmented lagrangian method for total variation video restoration," *IEEE Trans. Image Processing*, 2011.

[9] K. He, J. Sun, and X. Tang, "Guided image filtering," in *ECCV*, 2010, pp. 1–14.

[10] Y. Wang, W. Yin J. Yang, and Y. Zhan, "A new alternating minimization algorithm for total variation image reconstruction," *SIAM Journal on Imaging Sciences*, vol. 1(3), pp. 248–272, 2008.

[11] T.F. Chan and C.-K. Wong, "Total variation blind deconvolution," *IEEE Trans. on Image Processing*, vol. 7, no. 3, pp. 370–375, 1998.

[12] J.M. Bioucas-Dias and M.A.T. Figueiredo, "A new twist: Two-step iterative shrinkage/ thresholding algorithms for image restoration," *IEEE Trans. Image Processing*, vol. 16(12), pp. 2992–3004, 2007.